Electronic Supplementary Material (ESI) for Journal of Materials Chemistry A.

Copperohydrogel as a chemosensor for selective detection of oxometalate anions in water

Hamid Reza Khavasi and Elham Jelokhani*

Department of Inorganic Chemistry and Catalysis, Shahid Beheshti University, General Campus, Evin, Tehran 1983963113, Iran.

Email: h-khavasi@sbu.ac.ir

CORRESPONDING AUTHOR FOOTNOTE: Hamid Reza Khavasi, Tel No: +98 21 29903105, Fax No: +98 21 22431661.

Materials and methods

General. Starting materials and solvents were purchased from commercial sources and used as received. Infrared spectra (4000–250 cm^{-1}) of solid sample were recorded on a BOMEM-MB102 spectrometer as 1% dispersion in CsI pellets. Elemental analysis was performed using a Heraeus CHN-O Rapid analyzer. Melting points were obtained by a Bamstead Electrothermal type 9200 melting point apparatus and corrected. The ^{1}H NMR spectrum was recorded on a Bruker AC-300 MHz spectrometer at ambient temperature in DMSO-d_6. ^{1}H and ^{13}C NMR chemical shifts were referenced with respect to δ(TMS) = 0 ppm. Mass spectra were obtained on an Agilent mass spectrometer with 5973 Network Mass Selective Detector model in electron impact (70 eV) mode and quadruple analyser.

Synthesis of ligand. The ligand is conveniently prepared in a one pot synthesis procedure according to methods described previously.[S1] 2-Acetylpyridine (4.84 g, 40 mmol) was added into a solution of 3,4-di-methoxy benzaldehyde (3.32 g, 20 mmol) in EtOH (100 mL). KOH pellets (3.08 g, 85%, 40 mmol) and aq NH_3 (58 mL, 29.3%, 50 mmol) were then added to the solution. The solution was stirred at r.t. for 4 h. The off-white solid was collected by filtration and washed with EtOH (3×10 mL).]. Yield 55%, m.p=190°C. Anal. Calcd.: C, 74.78; H, 518; N, 11.37. Found: C, 74.81; H, 5.22; N, 11.40, FT-IR (cm^{-1}): 3317, 3054, 2236, 1679, 1587, 1468, 1390, 990, 880,731. ^{1}H NMR (300 MHz, DMSO-d_6), Figure S14: δ = 3.85 ($3H_{methoxy}$, s), 3.92 ($3H_{methoxy}$, s), 7.17 ($1H_{Ar}$, d, J = 9.0 Hz), 7.40-7.60 ($4H_{Ar}$, m), 7.95-8.10 ($2H_{Ar}$,m), 8.62-8.72 ($4H_{Ar}$,m), 8.73-8.83 ($2H_{Ar}$, m); ^{13}C NMR (400 MHz, DMSO-d_6), Figure S15: δ = 155.0, 154.6, 149.6, 148.9, 148.8, 136.8, 129.5, 123.9, 120.4, 119.1, 117.1, 116.7, 109.6, 55.2, and 55.1. MS m/z calcd for $[M]^{+}$ $(C_{23}H_{19}N_3O_2)^{+}$: 369.42; found 369.4.

Synthesis of pincer-type Cu(II) Complex: A solution of 10 mmol of ligand in 5 mL methanol and dichloromethane mixture (1:1) was added to a solution of 10 mmol of copper(II)chloride in 5 mL methanol and dichloromethane mixture (1:1) and then heated at 50 °C for 5 min. Green precipitate was collected by filtration and purified by recrystallization in methanol. Yield 71%, m.p=decomposed at 200°C. Anal.

Calcd.: C, 54.82; H, 3.80; N, 8.34. Found: C, 54.85 H, 3.83; N, 8.37. FT-IR (cm^{-1}): 3359, 3051, 2233, 1586, 1399, 1017, 799. MS m/z calcd for $[M\text{-}Cl]^+$ $(C_{23}H_{19}CuClN_3O_2)^+$: 468.41; found 468.4.

Preparation of the Gels: The elucidated green solution was achieved by dissolving of 3.2 mg of this complex in 1 ml water under heating. The stable metallogel was formed by cooling of this solution to ambient temperature.

Crystallization of Complexes: Suitable crystals for X-ray diffraction experiment is obtained from slow evaporation of methanol solution.

Single crystal diffraction studies. For crystal of copper complex intensity data were collected using a STOE IPDS-2T diffractometer with graphite monochromated Mo Kα radiation (λ) 0.71073 (Å). Data were collected in an a series of ω scans in 1° oscillations and integrated using the Stöe X-AREA[S2] software package. A numerical absorption correction was applied using the X-RED2[S3] and X-SHAPE[S4] software's. All structures were solved by direct methods using SHELXS-97[S5] and refined with full-matrix least-squares on F^2 using the SHELXL-97 program package. All non-hydrogen atoms were refined anisotropically. Hydrogen atoms were added at ideal positions and constrained to ride on their parent atoms, with U_{iso}(H) = 1.2Ueq. All refinements were performed using the X-STEP32 crystallographic software package.[S6] Structural illustrations have been drawn with ORTEP-3[S7] and MERCURY.[S8] Crystallographic data for compound 1 have been listed in Table S1.

REFERENCES:

[S1] Wang, J.; Hanan, G. A Facile Route to Sterically Hindered and Non-Hindered 4′-Aryl-2,2′:6′,2″-Terpyridines. *Synlett* **2005**, *8*, 1251–1254.

[S2] Stoe, C. X–AREA: Program for the Acquisition and Analysis of Data, Version 1.30. *Stoe Cie GmbH Darmatadt, Ger.* **2005**.

[S3] X–RED: Program for Data Reduction and Absorption Correction, vesion 1.28b: Stoe & Cie GmbH:

Darmstadt, Germany, 2005. *No Title*.

[S4] X–SHAPE: Program for crystal optimization for numerical absorption correction, vesion 2.05: Stoe & Cie GmbH: Darmstadt, Germany, 2004. No TitleX–SHAPE: Program for Crystal Optimization for Numerical Absorption Correction, Vesion 2.05: Stoe & Cie GmbH: Darmstadt, Germany, 2004.

[S5] Sheldrick, G. M. SHELX-97, Program for the Solution and Refinement of Crystal Structures. *Univ. Göttingen, Ger.* **1997**.

[S6] Stoe, C. X-STEP32, Version 1.07 b, Crystallographic Package. *Stoe Cie GmbH, Darmstadt, Ger.* **2000**.

[S7] Farrugia, L. J.; IUCr. *WinGX* and *ORTEP for Windows* : An Update. *J. Appl. Crystallogr.* **2012**, *45* (4), 849–854.

[S8] Mercury 3.10.1 Supplied with Cambridge Structural Database; CCDC: Cambridge, U.K., 2017−2018. Mercury 3.10.1 Supplied with Cambridge Structural Database; CCDC: Cambridge, U.K., 2017−2018No Title.

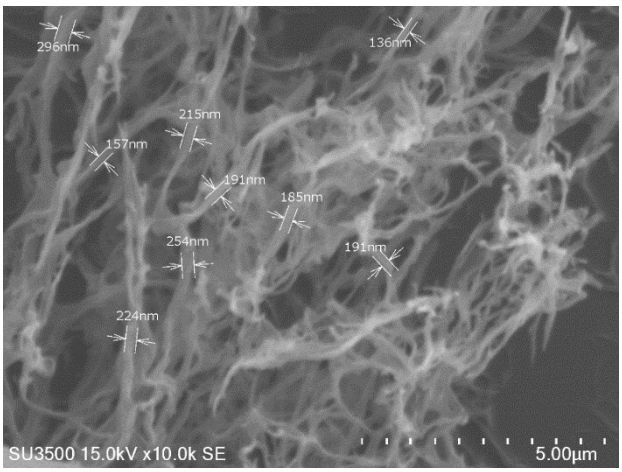

Figure S1. SEM image of the vacuum dried gel, xerogel, formed from the gel obtained by dissolution of the ligand and $CuCl_2$ salt in water.

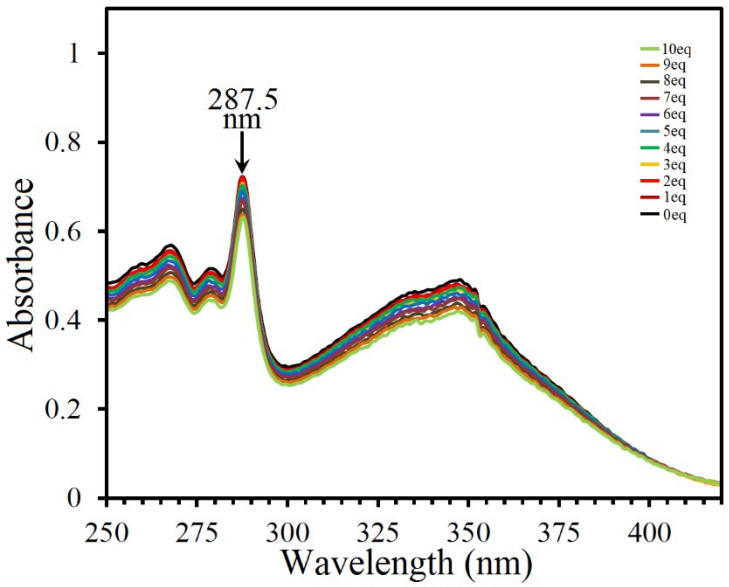

Figure S2. UV-vis spectral changes observed for [$CuCl_2{L^{3,4(OMe)2-phen}_{Terpy}}$] metal complex ($2.8\times10^{-5}$ M) upon addition of sodium salt of Cl^- anion in water. Arrow indicates the absorption band decreases during the titration.

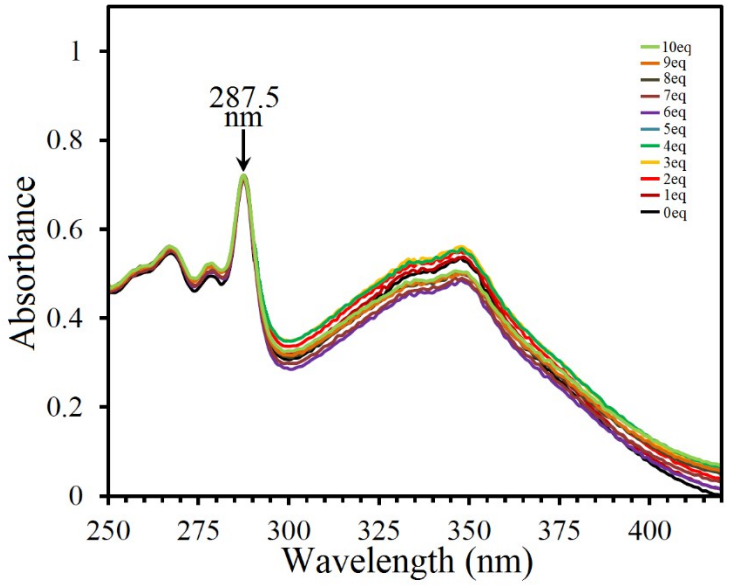

Figure S3. UV-vis spectral changes observed for [$CuCl_2L^{3,4(OMe)2-phen}_{Terpy}$] metal complex ($2.8\times10^{-5}$ M) upon addition of sodium salt of Br^- anion in water. Arrow indicates the absorption band decreases during the titration.

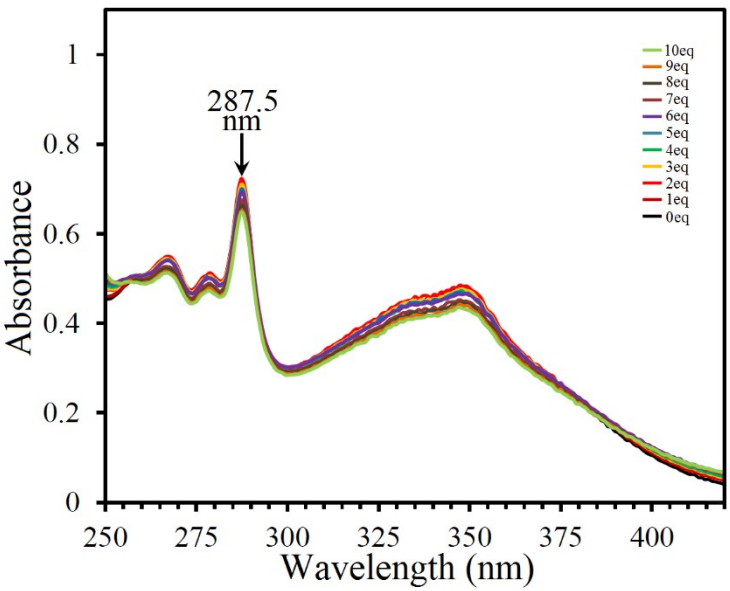

Figure S4. UV-vis spectral changes observed for [$CuCl_2L^{3,4(OMe)2-phen}_{Terpy}$] metal complex ($2.8\times10^{-5}$ M) upon addition of sodium salt of I^- anion in water. Arrow indicates the absorption band decreases during the titration.

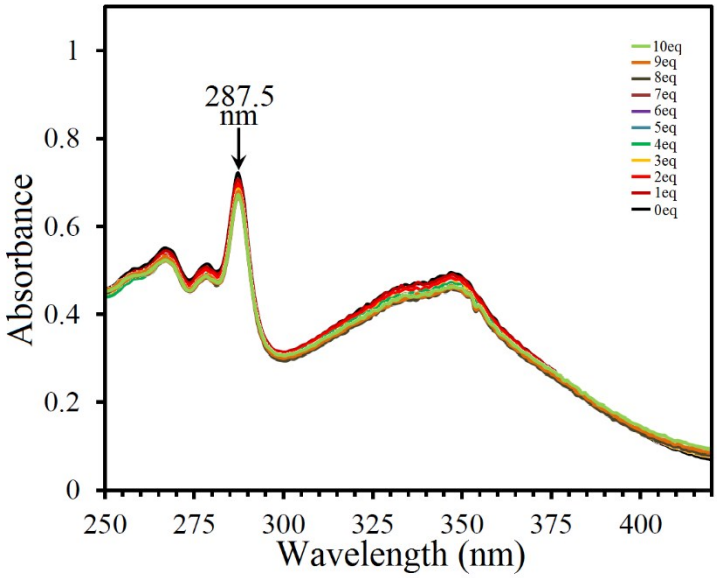

Figure S5. UV-vis spectral changes observed for [$CuCl_2L^{3,4(OMe)2-phen}_{Terpy}$] metal complex ($2.8\times10^{-5}$ M) upon addition of sodium salt of NO_2^- anion in water. Arrow indicates the absorption band decreases during the titration.

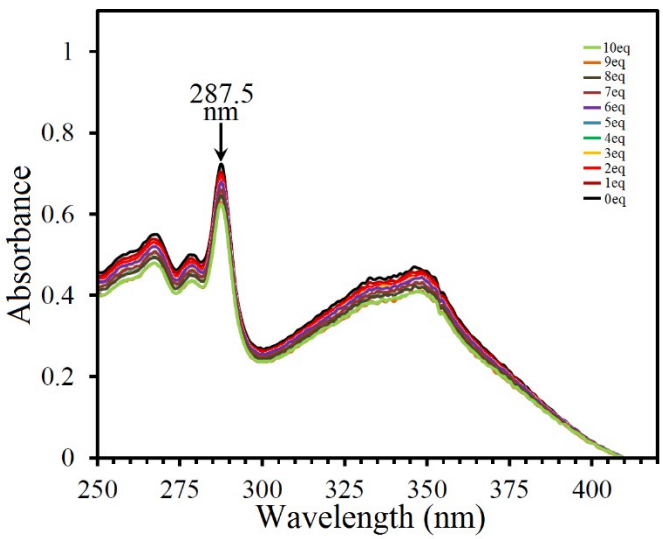

Figure S6. UV-vis spectral changes observed for [$CuCl_2L^{3,4(OMe)2-phen}_{Terpy}$] metal complex ($2.8\times10^{-5}$ M) upon addition of sodium salt of NO_3^- anion in water. Arrow indicates the absorption band decreases during the titration.

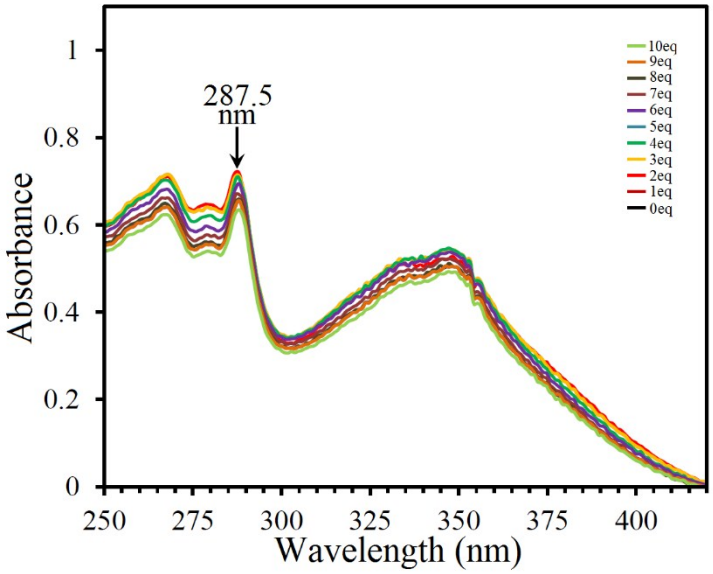

Figure S7. UV-vis spectral changes observed for [$CuCl_2L^{3,4(OMe)2-phen}_{Terpy}$] metal complex ($2.8\times10^{-5}$ M) upon addition of sodium salt of PO_4^{3-} anion in water. Arrow indicates the absorption band decreases during the titration.

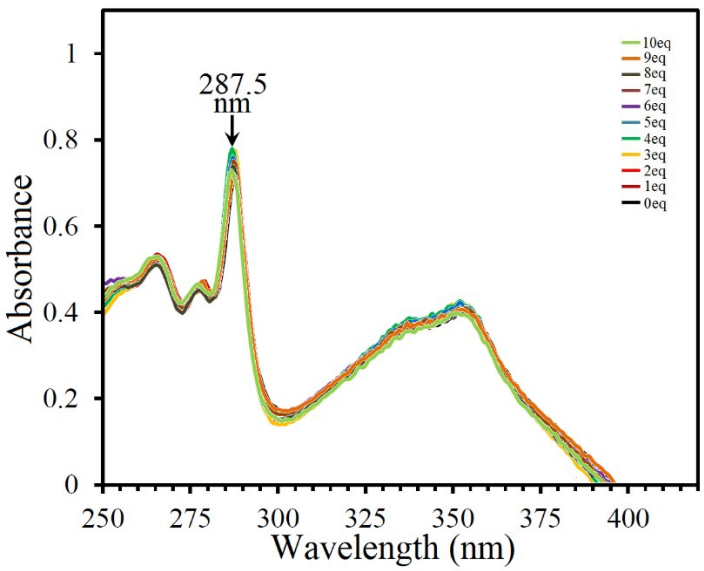

Figure S8. UV-vis spectral changes observed for [$CuCl_2L^{3,4(OMe)2-phen}_{Terpy}$] metal complex ($2.8\times10^{-5}$ M) upon addition of sodium salt of SO_3^{2-} anion in water. Arrow indicates the absorption band decreases during the titration.

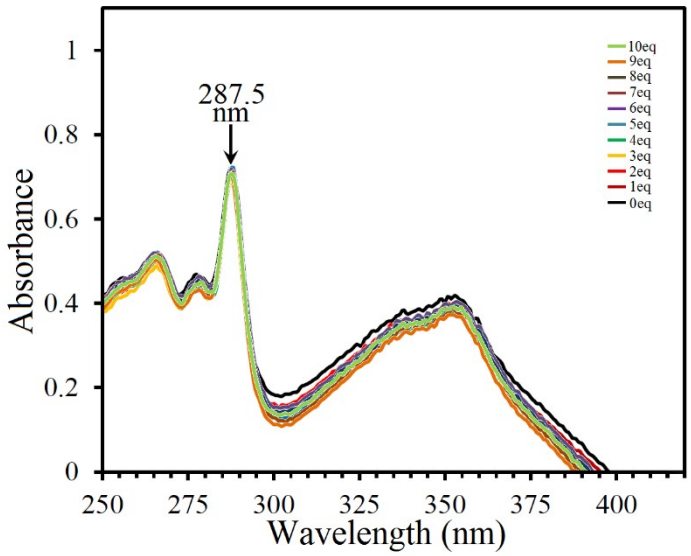

Figure S9. UV-vis spectral changes observed for [$CuCl_2L^{3,4(OMe)2-phen}_{Terpy}$] metal complex ($2.8\times10^{-5}$ M) upon addition of sodium salt of SO_4^{2-} anion in water. Arrow indicates the absorption band decreases during the titration.

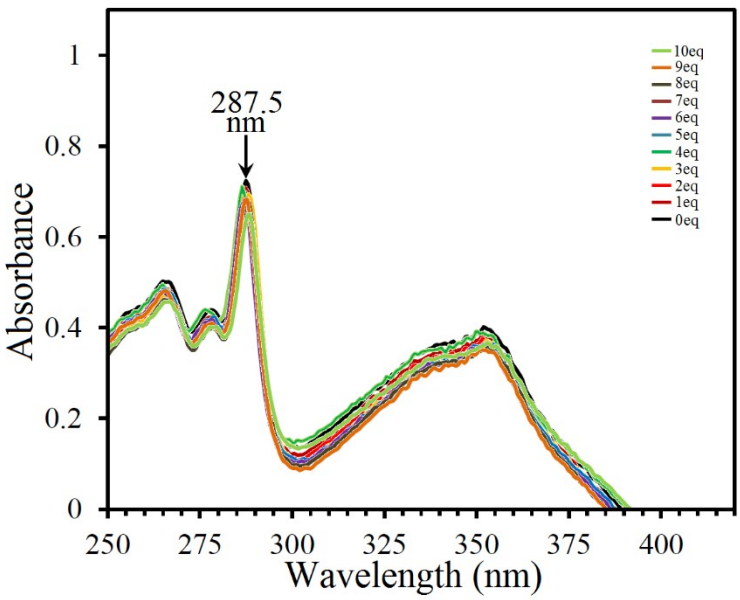

Figure S10. UV-vis spectral changes observed for [$CuCl_2L^{3,4(OMe)2-phen}_{Terpy}$] metal complex ($2.8\times10^{-5}$ M) upon addition of sodium salt of ClO_4^- anion in water. Arrow indicates the absorption band decreases during the titration.

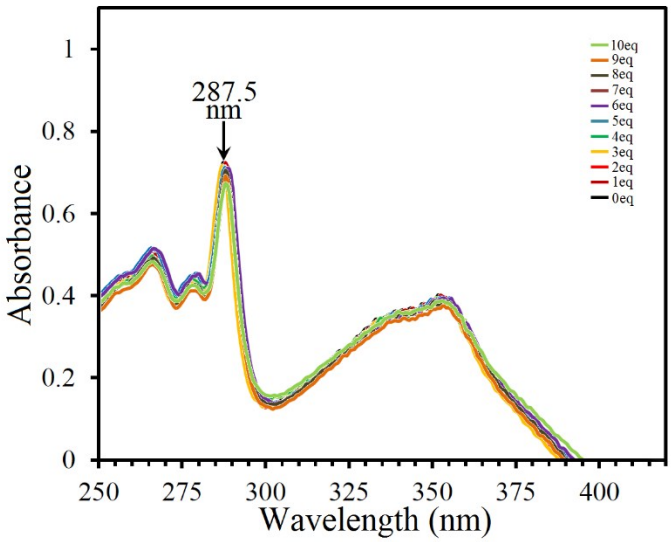

Figure S11. UV-vis spectral changes observed for [$CuCl_2L^{3,4(OMe)2-phen}_{Terpy}$] metal complex ($2.8\times10^{-5}$ M) upon addition of sodium salt of HSO_3^- anion in water. Arrow indicates the absorption band decreases during the titration.

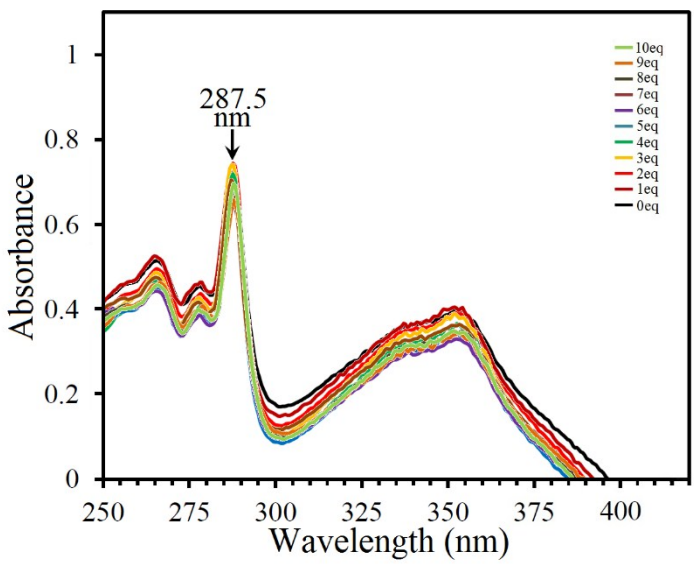

Figure S12. UV-vis spectral changes observed for [$CuCl_2L^{3,4(OMe)2-phen}_{Terpy}$] metal complex ($2.8\times10^{-5}$ M) upon addition of sodium salt of CN^- anion in water. Arrow indicates the absorption band decreases during the titration.

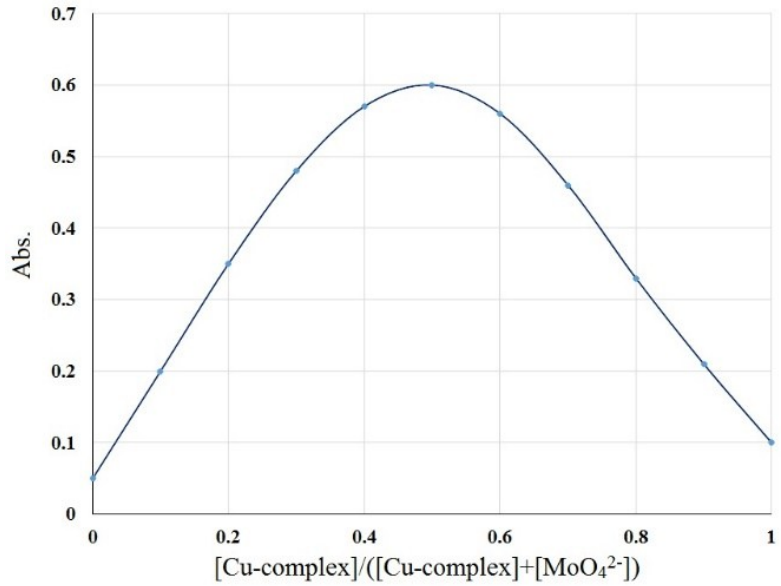

Figure S13. Job plot receptor of [$CuCl_2L^{3,4(OMe)2-phen}_{Terpy}$] metal complex with MoO_4^{2-} anion at 287.5 nm. The total concentration of the host and guest was 2.8×10^{-5} M.

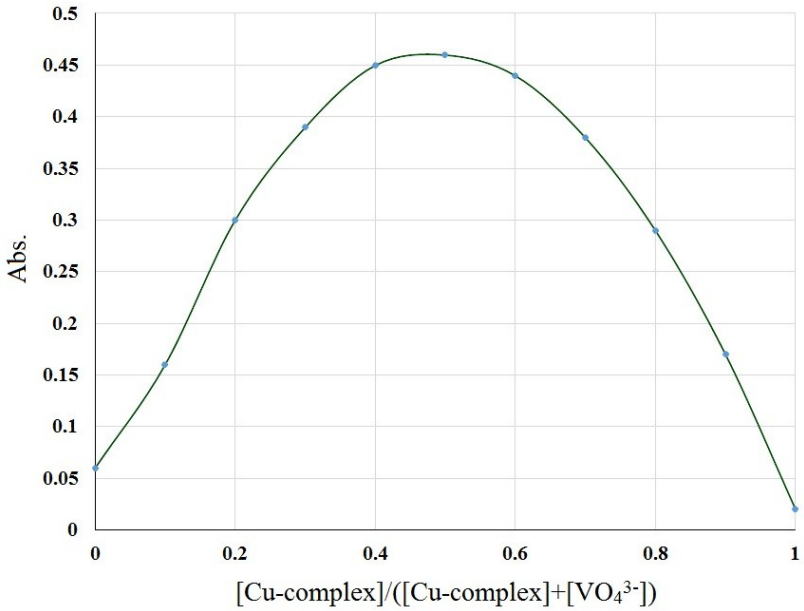

Figure S14. Job plot receptor of [$CuCl_2L^{3,4(OMe)2-phen}_{Terpy}$] metal complex with VO_4^{3-} anion at 287.5 nm. The total concentration of the host and guest was 2.8×10^{-5} M.

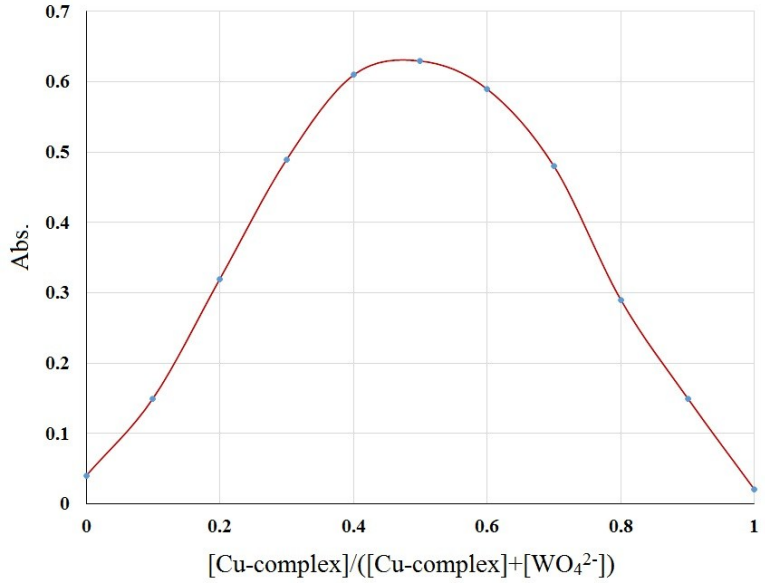

Figure S15. Job plot receptor of [$CuCl_2L^{3,4(OMe)2-phen}_{Terpy}$] metal complex with WO_4^{2-} anion at 287.5 nm. The total concentration of the host and guest was 2.8×10^{-5} M.

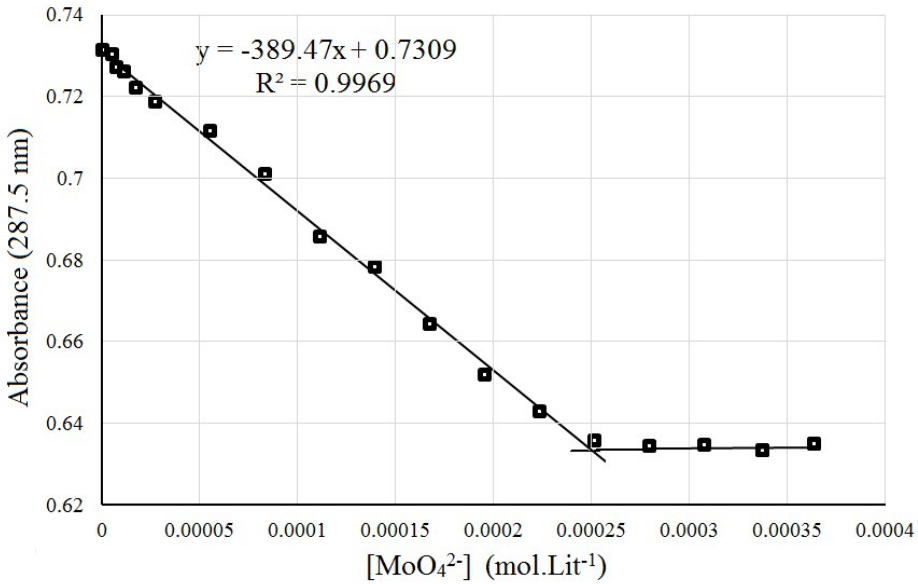

Figure S16. The plot of absorbance (at 287.5 nm) changes of aqueous solution of [$CuCl_2L^{3,4(OMe)2-phen}_{Terpy}$] metal complex ($2.8\times10^{-5}$ M) against addition of aqueous solution of MoO_4^{2-} anion.

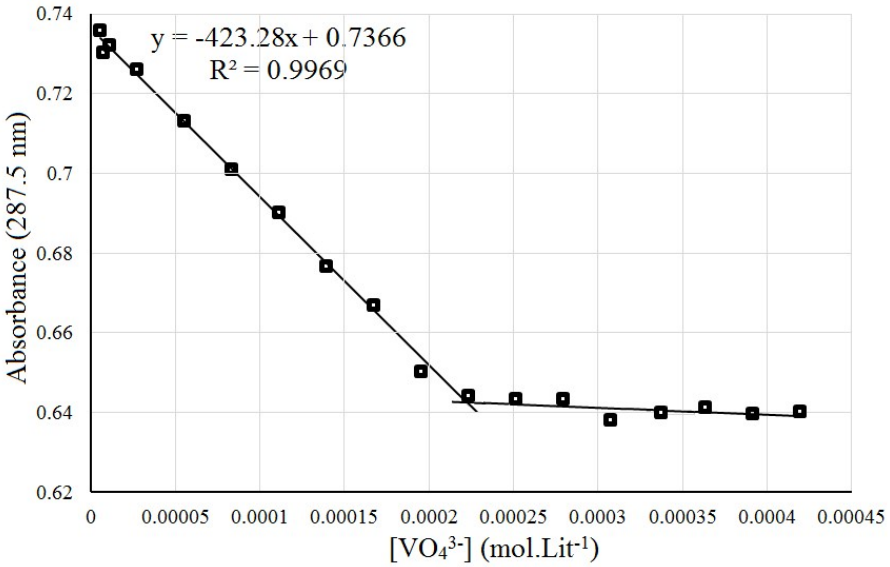

Figure S17. The plot of absorbance (at 287.5 nm) changes of aqueous solution of [$CuCl_2L^{3,4(OMe)2-phen}_{Terpy}$] metal complex ($2.8\times10^{-5}$ M) against addition of aqueous solution of VO_4^{3-} anion.

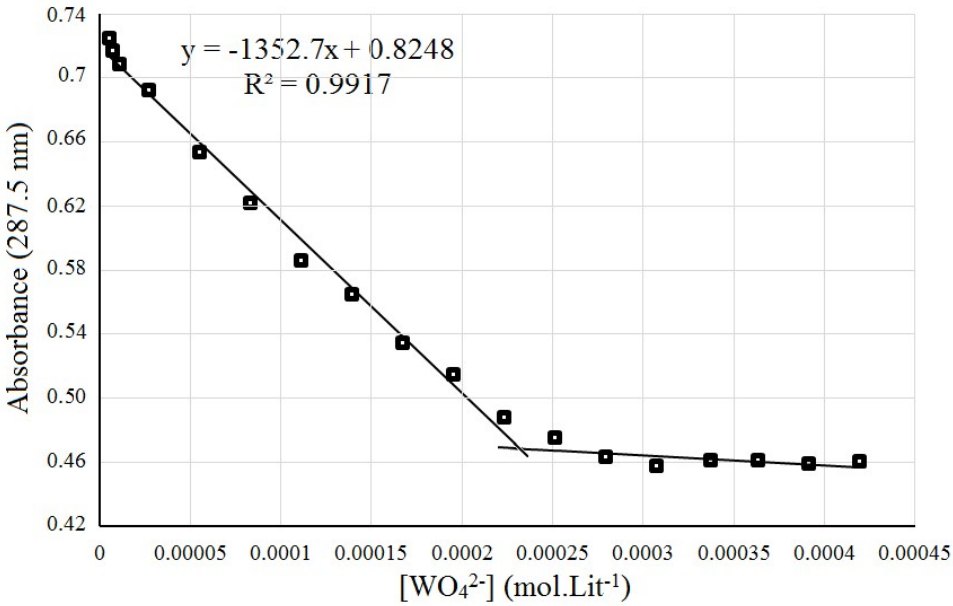

Figure S18. The plot of absorbance (at 287.5 nm) changes of aqueous solution of [$CuCl_2L^{3,4(OMe)2-phen}_{Terpy}$] metal complex ($2.8\times10^{-5}$ M) against addition of aqueous solution of WO_4^{2-}anion.

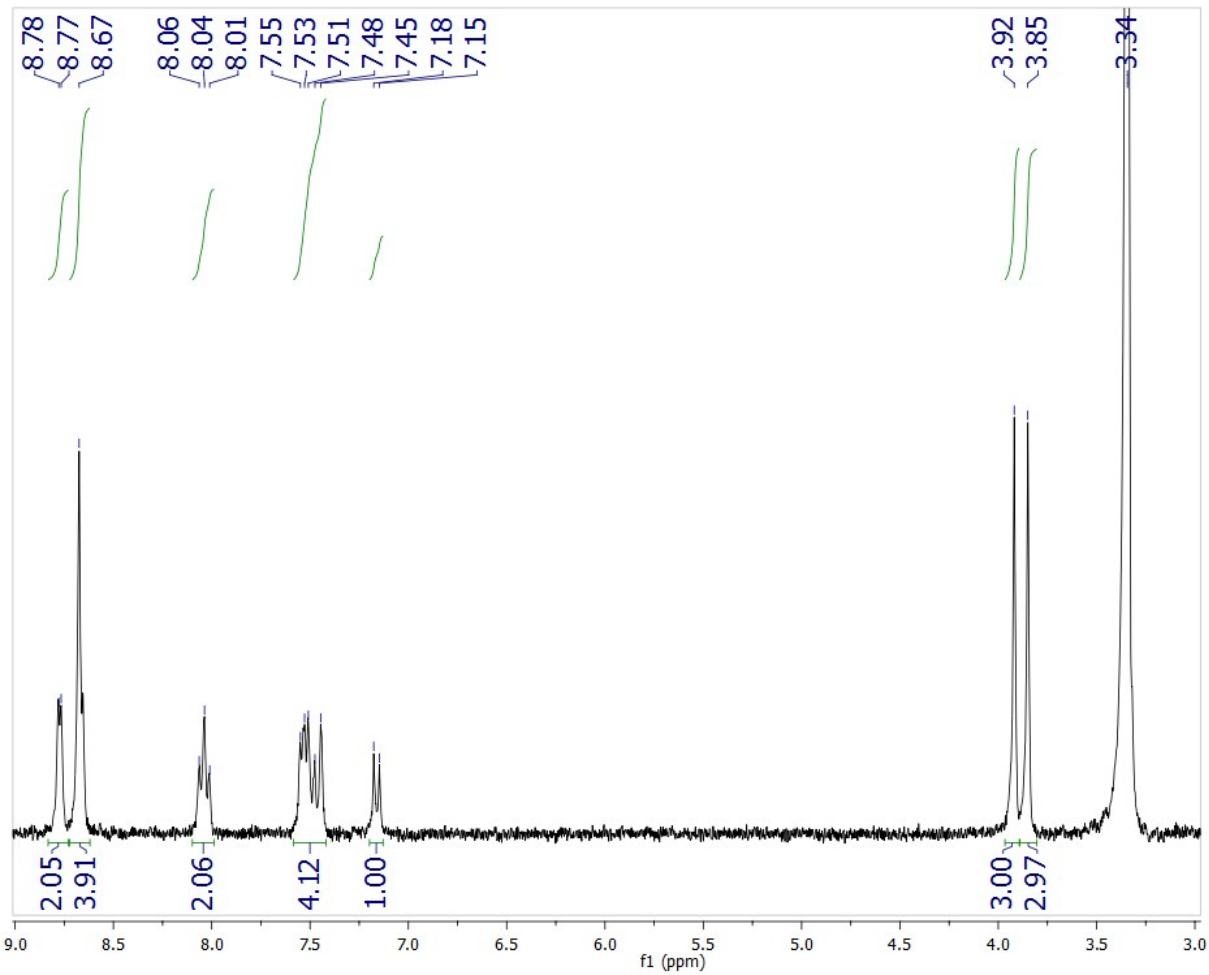

Figure S19. ^{1}H NMR spectrum of 4'-(3,4-dimethoxy-phenyl)-[2,2';6',2"]terpyridine, $L^{3,4(OMe)2-phen}_{Terpy}$, was recorded on a Bruker AC-300 MHz spectrometer at ambient temperature in DMSO-d_6. The chemical shifts were referenced with respect to δ(TMS) = 0 ppm.

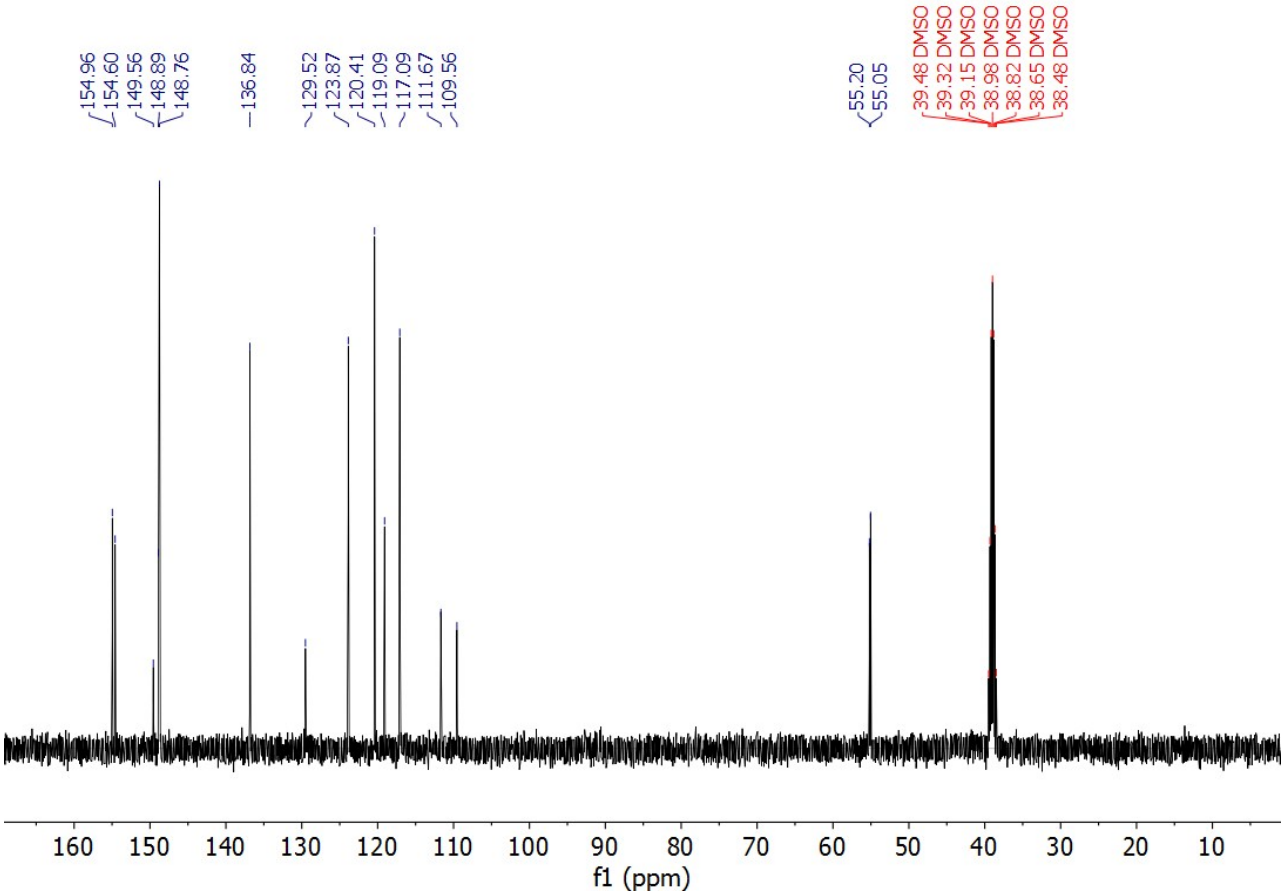

Figure S20. ^{13}C NMR spectrum of 4'-(3,4-dimethoxy-phenyl)-[2,2';6',2'']terpyridine, $L^{3,4(OMe)2-phen}_{Terpy}$, was recorded on a Bruker AC-300 MHz spectrometer at ambient temperature in DMSO-d_6. The chemical shifts were referenced with respect to δ(TMS) = 0 ppm.

Table S1. Crystal data and structural refinement for copper complex of [$CuCl_2L^{3,4(OMe)2-phen}_{Terpy}$].

	[$CuCl_2L^{3,4(OMe)2-phen}_{Terpy}$]
formula	$C_{23}H_{19}Cl_2CuN_3O_2$
fw	503.86
λ/Å	0.71073
T/K	298(2)
crystal.system	Monoclinic
space group	*C*2/*c*
a/Å	25.287(4)
b/Å	14.2223(18)
c/Å	13.780(2)
β/°	121.338(9)
V/Å^3	4233.0(10)
ρ_{calc}g/cm^3	1.581
Z	8
μ/mm^{-1}	1.311
F(000)	2056
2θ/°	54.00
R(int)	0.0712
GOOF	1.012
R_1[a]($I > 2\sigma(I)$)	0.0690
wR_2[b]($I > 2\sigma(I)$)	0.1379
CCDC No.	1873052

[a]$R_1 = \Sigma||F_o| - |F_c||/\Sigma|F_o|$. [b]$wR_2 = [\Sigma(w(F_o^2 - F_c^2)^2)/\Sigma w(F_o^2)2]^{½}$.

Table S2. Coordination geometry, dimensionality and aromatic interaction parameters (Å and °) for description of π-π interaction in complex [$CuCl_2L^{3,4(OMe)2-phen}_{Terpy}$].

Cg(I)-Cg(J)	$d_{Cg\text{-}Cg}$[a]	α[b]	β, γ[c]	$d_{plane\text{-}plane}$[d]	d_{offset}[e]
Cg(1)-Cg(2)[i]	3.750	8.74	25.53, 16.80	3.590, 3.384	1.084, 1.616
Cg(1)-Cg(2)[ii]	3.664	2.71	20.23, 17.73	3.490, 3.438	0.304, 0.346

[a] Centroid-centroid distance. [b] Dihedral angle between the ring plane. [c] Offset angles: angle between Cg(I)–Cg(J) vector and normal to plane I, angle between Cg(I)-Cg(J) vector and normal to plane J ($\beta = \gamma$ when $\alpha = 0$). [d] Perpendicular distance of Cg(I) on ring J and perpendicular distance of Cg(J) on ring I. [e] Horizental displacement between Cg(I) and Cg(J), two values if the two rings are not exactly parallel ($\alpha \neq 0$). Cg(1): centroid of N(2)-C(6)-C(7)-C(8)-C(9)-C(10), and Cg(2): centroid of N3(7)-C(11)-C(12)-C(13)-C(14)-C(15). Symmetry codes: (i) 1-x, y, 3/2-z, and (ii) 1-x, 1-y, 1-z.

Table S3. Hydrogen bonding parameters (Å and °) for complex [$CuCl_2L^{3,4(OMe)2-phen}_{Terpy}$].

Compound	D-H···A	d(D-H)	d(H···A)	d(D···A)	<(DHA)	Symmetry codes
[$CuCl_2L^{3,4(OMe)2-phen}_{Terpy}$]	C9-H9…Cl2	0.930	2.780	3.655(6)	157.2	1-x, 1-y, 1-z
	C12-H12…Cl2	0.930	2.613	3.500(7)	159.7	1-x, 1-y, 1-z
	C9-H9...Cl2	0.930	2.884	3.797(5)	167.4	1-x, 1-y, 1-z
	C20-H20...Cl1	0.930	2.854	3.516(6)	129.2	1/2+x, 3/2-y, 1/2+z
	C22-H22...Cl2	0.960	2.874	3.473(7)	121.1	1-x, 1-y, 1-z
	C23-H23C… Cl2	0.930	2.942	3.690(8)	135.7	3/2-x, -1/2+y, 3/2-z

Table S4. Geometrical parameters (Å and °) for the description of the Cu−Cl···π interaction in complex [$CuCl_2L^{3,4(OMe)2-phen}_{Terpy}$].

	Cu-Cl...π[#1]	**Definition of geometrical Cu-Cl…π parameters**
r_r (Å)[a]	3.611	
r_a (Å)[a]	3.344(8) (C5)	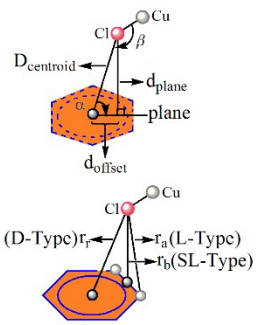
r_b (Å)[a]	3.385	
$D_{centroid}$ (Å)[b]	3.611	
d_{plane} (Å)[c]	3.341	
d_{offset} (Å)[d]	1.370	
α (°)[e]	67.7	
β (°)[f]	109.47	
Type[g]	L	
Sym. code	#1: 1-x, y, 3/2-z	

[a]r_i is the shortest distance between the halogen and ring member atom, (r_a), bond, (r_b), or centroid of the ring atoms, Cg, (r_r). [b]$D_{centroid}$ is the halogen distance from the centroid of ring atoms. [c]d_{plane} is the distance between halogen atom and the ring plane. [d]d_{offset} is the parameter which determines displacement of the halogen from the centre of the aromatic ring, [$d_{offset} = (D_{centroid}^2 - d_{plane}^2)^{1/2}$]. [e]$\alpha$ is angle between $D_{centroid}$ and d_{offset} vectors. [f]β is Zn-X-Cg angle. [g]Localized, delocalized and semi-localized Cu-Cl...π interactions are abbreviated by L-type, D-type and SL-type, respectively.